haematologica
Journal of the Ferrata Storti Foundation

Multi-omics analysis reveals a unique epigenetic signature in MYD88 wild-type Waldenstrom macroglobulinemia

by Karan Chohan, Jonas Paludo, Surendra Dasari, Joseph P. Novak, Jithma P. Abeykoon, Saurabh Zanwar, Zhi-Zhang Yang, Shahrzhad Jalali, Vaishali Bhardwaj, Jordan E. Krull, Esteban Braggio, Michelle K. Manske, Craig B. Reeder, Sikander Ailawadhi, Asher Chanan-Khan, Prashant Kapoor, Robert A. Kyle, Morie A. Gertz, Anne J. Novak, Patrizia Mondello and Stephen M. Ansell

Received: August 28, 2025.
Accepted: November 24, 2025.

Citation: Karan Chohan, Jonas Paludo, Surendra Dasari, Joseph P. Novak, Jithma P. Abeykoon, Saurabh Zanwar, Zhi-Zhang Yang, Shahrzhad Jalali, Vaishali Bhardwaj, Jordan E. Krull, Esteban Braggio, Michelle K. Manske, Craig B. Reeder, Sikander Ailawadhi, Asher Chanan-Khan, Prashant Kapoor, Robert A. Kyle, Morie A. Gertz, Anne J. Novak, Patrizia Mondello and Stephen M. Ansell. Multi-omics analysis reveals a unique epigenetic signature in MYD88 wild-type Waldenstrom macroglobulinemia. Haematologica. 2025 Dec 4. doi: 10.3324/haematol.2025.289068 [Epub ahead of print]

Multi-omics analysis reveals a unique epigenetic signature in *MYD88* wild-type Waldenstrom macroglobulinemia

Karan Chohan[1#], Jonas Paludo[1#], Surendra Dasari[2], Joseph P Novak[1], Jithma P. Abeykoon[1], Saurabh Zanwar[1], Zhi-Zhang Yang[1], Shahrzad Jalali[1], Vaishali Bhardwaj[1], Jordan E Krull[1], Esteban Braggio[3], Michelle K. Manske[1], Craig B. Reeder[4], Sikander Ailawadhi[4], Asher Chanan-Khan[4], Prashant Kapoor[1], Robert A. Kyle[1], Morie A Gertz[1], Anne J. Novak[1], Patrizia Mondello[1] and Stephen M. Ansell[1]*

[1]Division of Hematology, Mayo Clinic, Rochester, MN, USA

[2]Department of Health Sciences Research, Mayo Clinic, Rochester, MN, USA

[3]Division of Hematology and Medical Oncology, Mayo Clinic, Scottsdale, AZ, USA

[4]Division of Hematology and Oncology, Mayo Clinic, Jacksonville, FL, USA

#Authors contributed equally

Correspondence:

Stephen M. Ansell, M.D., Ph.D.

200 1st ST SW, Rochester, MN, USA, 55902

Email: ansell.stephen@mayo.edu; Phone: (507)-284-2511

Running Header: Epigenetic Analysis of *MYD88*-WT WM

Data Sharing Statement: RNA data are available at GEO under the accession numbers: GSE232994 and GSE232995. Methylation data are available on Zenodo under the record number: 11206554. For additional data on the patients, please contact the corresponding author.

Acknowledgements:

This study was supported by research funding from the BINK Foundation, and the International Waldenstrom Macroglobulinemia Foundation (IWMF) to SMA and the Mayo Clinic.

Author Contributions:

KC, JP, SD, SMA designed this study, analyzed/interpreted the data, and wrote the manuscript. JPN, JPA, SZ, ZY, SJ, VB, JEK, EB, MKM, AP, CBR, SA, AC, PK, RAK, MAG, AJN, PM, interpreted the data and assisted in writing the manuscript. All authors provided final approval of the manuscript and are accountable for all aspects of the work.

Conflict of Interest Disclosures:

S.M.A receives research funding from: Bristol-Myers Squibb, Seattle Genetics, Affimed Therapeutics, Regeneron, Trillium Therapeutics, AI Therapeutics, ADC Therapeutics. PM is supported by the NCI K08CA279652, LRF Clinical Investigator Award (CDA 1020588), the Gerstner Family Career Development Award, the ASH Junior Faculty Scholar Award, the

IWMF/LLS Strategic Research Roadmap Initiative, and the IWMF/LLS Enhanced Research Roadmap Initiative. All remaining authors declare no competing conflict-of-interests.

Supplemental Material: 1 Supplemental Table

Keywords: Waldenstrom macroglobulinemia; MYD88; epigenetics; DNA methylation; microRNAs.

MYD88 L265P mutations (MUT) are found in approximately 90% of patients with Waldenstrom macroglobulinemia (WM) and lead to the activation of pro-survival signaling (1, 2). Prior literature has demonstrated that patients with *MYD88* wild-type (WT) WM have inferior responses to conventional therapies and a higher likelihood of histological transformation to an aggressive lymphoma (3). Increasingly, the role of non-coding genomics in lymphomagenesis has demonstrated importance and currently, the epigenetic landscape of *MYD88*^{WT} WM remains largely underexplored (4). Previously, our group showed how DNA methylation and non-coding RNAs may alter the control of critical genes which may be responsible for the progression of IgM-monoclonal gammopathy to WM disease (5-7). Given the demonstrated importance of these non-coding epigenetic regulators, the aim of this study was to utilize a multi-omics approach to assess the role of microRNAs (miRNAs) and DNA methylation in driving *MYD88*^{WT} WM biology through comparison with *MYD88*^{MUT} WM patients and healthy controls.

Bone marrow samples were prospectively collected from 20 subjects [3 *MYD88*^{WT}/*CXCR4* ^{WT} WM, 12 *MYD88*^{MUT} WM (three had *CXCR4* mutated disease), and 5 healthy controls]. WM was defined as ≥10% BM involvement by lymphoplasmacytic lymphoma and serum IgM monoclonal protein of any size. Positive selection for CD19+ and/or CD138+ B cells was performed on samples utilizing STEMCELL CD19+ and CD138+ selection kits (17854, 17877). Clonal sorting was not performed. Analyses were conducted as per prior reports and focused on comparisons between *MYD88*^{WT} WM to normal controls and *MYD88*^{WT} to *MYD88*^{MUT} WM (5-7). Briefly, RNA differential expression for miRNAs and mRNAs was conducted using a $\log_2$ fold change (FC)>0.5 or <-0.5 and false discovery rate (FDR)<0.05. Genome-wide DNA methylation analysis was performed, and CpG methylation ratios were segmented into 200-bp regions. Differentially methylated regions (DMRs) were determined using a Q-value <0.05 and an absolute methylation difference ≥10%. The ≥10% absolute methylation difference was established after investigation of different threshold values, as it allowed sufficient identification of DMRs while effectively reducing background noise. Next, RNA-seq data from matched samples were integrated to the methylome and analyzed to identify differentially expressed genes ($\log_2$FC>0.5 or <-0.5, FDR<0.05) with corresponding promoter hypo- or hypermethylated DMR. For miRNA analysis, miRNA-mRNA target analysis was performed, and differentially expressed miRNA-mRNA pairs with a correlated biological expression (i.e., either upregulated miRNA experimentally predicted to regulate downregulated mRNA or *vice versa)* were selected. The Ingenuity Pathway Analysis (IPA) was used to determine potentially epigenetically regulated pathways using a corrected p<0.05. This study received approval from the Mayo Clinic Institutional Review Board (IRB).

Patient characteristics for the whole cohort and stratified by *MYD88* mutation status are included in **Table 1**. Baseline characteristics were comparable between *MYD88*^{MUT} and *MYD88*^{WT} WM patients. All *MYD88*^{WT} WM patients were *CXCR4*^{WT}, and three patients from the *MYD88*^{MUT} WM cohort were *CXCR4*^{MUT}. Characteristics from healthy control samples were not available per institutional policy.

Comparing *MYD88*^{WT} WM samples to controls, a greater number of hypermethylated DMRs were observed across genomic regions (hyper- vs hypomethylated): promoter (29129 vs 6300), 3'untranslated region (UTR) (2068 vs 1551), 5'UTR (10169 vs 735), intron (30344 vs 24511), exon (22224 vs 6855), CpG island (30372 vs 1240) and CpG shore (14477 vs 5872) (all p<0.0001) (**Figure 1A**). Next, mRNA analysis demonstrated that 352 differentially expressed genes had concordant up-/downregulation with promoter hypo-/hypermethylated DMR.

On the assessment of promoter-methylation-based pathways, comparing *MYD88*^{WT} WM to controls, multiple pathways involved in cell signaling, proliferation, gene regulation, cytokine and immune signaling, and metabolism were found to be differentially regulated (**Figure 1B**). Most pathways were observed to be negatively enriched, including several members of interleukin (IL) signaling (IL-2, IL-3, IL-7) and regulators of cell proliferation and signaling, including mTOR, PI3K/AKT, and p53. Underlying multiple pathways were promoter hypermethylation and mRNA downregulation of *AKT3*, *MAP3K1*, and *PIK3CA* genes.

Next, methylation studies comparing *MYD88*^{WT} to *MYD88*^{MUT} WM samples demonstrated a similar hypermethylated profile in *MYD88*^{WT} with statistically greater number of hypermethylated DMRs observed across genomic regions (hyper- vs hypomethylated): promoter (24829 vs 2544), 3'untranslated region (UTR) (3534 vs 378), 5'UTR (6111 vs 605), intron (52292 vs 5360), exon (21066 vs 2187), CpG island (18334 vs 1551) and CpG shore (16351 vs 1957) (all $p<0.0001$) (**Figure 1C**). Assessing mRNA expression, 212 differentially expressed genes had concordant up-/downregulation with promoter hypo-/hypermethylated DMR.

Methylation-based pathway analysis comparing *MYD88*^{WT} to *MYD88*^{MUT} WM samples showed downregulation of cytokine signaling, including IL-8, IL-17, and regulators of intracellular signaling, including RAC (**Figure 1D**). Of note, we have previously demonstrated reduced levels of IL-8 in WM, and in the present analysis, we find hypermethylation with associated downregulation of the downstream RAS superfamily genes including, *RHOC* and *RRAS2* (**Figure 1E**) (8). Additionally, underlying multiple downregulated cytokine pathways (IL-8, IL-4, IL-13) was promoter hypermethylation with associated mRNA downregulation of *BCL2*, an important regulator of apoptosis, and a current therapeutic target in WM (9). In relation to RAC inactivation, we observed potential upstream inhibition of this pathway via promoter hypermethylation of the integrin genes *ITGAM* (integrin alpha M) and *ITGB1* (integrin beta 1), both found to be downregulated (10).

On miRNA analysis, comparing *MYD88*^{WT} WM to control samples, we observed 192 differentially expressed transcripts (70 downregulated; 122 upregulated) experimentally targeting 6255 mRNAs (**Figure 2A**). After target analysis and filtering, pathway analysis demonstrated multiple intracellular signaling, and metabolism pathways were downregulated (**Figure 2B**). Here, we observed miRNA-based downregulation of the RAC signaling pathway, a pathway also downregulated in our methylation analysis. Underlying this pathway was upregulation of miR-98-3p (FC: 2.4; FDR: <0.005) and let-7a-5p (FC: 1.1; FDR<0.005) targets of *PIK3C3* and *MAP3K1*, respectively, found to be downregulated. These targets are members of the PI3K/AKT and MAPK family, and prior reports have demonstrated the role of miR-98 in regulating tumor progression via targeting of these pathways (11). Relating back to our methylation analysis, we similarly observed downregulation of PI3K/AKT and MAPK signaling comparing *MYD88*^{WT} WM to controls (**Figure 1B**); thus, these findings indicate multiple epigenetic regulators may influence key intracellular signaling pathways that regulate cytokine and immune function.

In comparing *MYD88*^{WT} to *MYD88*^{MUT} WM samples, our miRNA analysis identified 11 differentially expressed transcripts (all downregulated) experimentally targeting 3011 differentially expressed mRNAs (**Figure 2C**). Here, pathway analysis revealed upregulation of chromatin organization and histone modification signaling (**Figure 2D**). Underlying both pathways was the downregulation of miR-138-5p (FC: -9.8; FDR: 0.015), which targets *DNMT3A* and *DOT1L*, both of which were observed to be upregulated on mRNA analysis. Of

relevance, miR-138-5p has been demonstrated to act as a tumor suppressor, and *DOT1L* is a histone methyltransferase involved in the regulation of mRNA transcription (12, 13). Furthermore, *DNMT3A* is a critical epigenetic regulator responsible for the addition of methyl groups at CpG sites; thus, upregulation of this gene corresponds with the CpG hypermethylation seen across genomic regions in *MYD88*^{WT} WM patients (**Figure 2E**) (14).

Overall, we identified for the first time a distinct epigenetic signature in *MYD88*^{WT} WM. An important limitation of this study is the smaller sample size of patients with *MYD88*^{WT} WM given the rarity of this diagnosis. To address this limitation, we sought to compare our findings with a previously published cohort of 18 patients with *MYD88*^{WT} disease (15). In this prior report, utilizing gene set enrichment analysis comparing *MYD88*^{WT} to *MYD88*^{MUT} WM patients, significant enrichment for the upregulation of E2F, MYC, PI3K-AKT-MTOR, and G2M checkpoint signaling targets and the downregulation of inflammatory response genes and TNFA signaling via NF-κB was found (15). Performing a similar mRNA-based gene set analysis comparing our *MYD88*^{WT} to *MYD88*^{MUT} WM samples, we observed a concordant pattern (**Supplemental Table 1**) with positive enrichment of E2F, MYC, MTOR and G2M checkpoint signaling, and negative enrichment of TNFA signaling via NF-κB and inflammatory response signaling (all $p<0.05$). These consistent patterns offer external support for the observations presented in the current study.

A central feature of our analysis of *MYD88*^{WT} WM patients was the epigenetic inactivation of cytokine and intracellular pathways involved in immune regulation, including the IL-8 and the PI3K/AKT/mTOR pathways. Although constitutional activation of MYD88 serves a critical role in the proinflammatory signaling observed in *MYD88*^{MUT} WM patients, these findings suggest that both methylation and miRNA-based mechanisms may epigenetically regulate the reduced inflammatory signaling in *MYD88*^{WT} WM beyond only the mutation in *MYD88* (1, 2). In relation to treatment, given that BTK inhibitor efficacy relies on suppression of activated inflammatory pathways, these findings also suggest a potential non-coding mechanism for the reduced response to BTKis in patients with *MYD88*^{WT} WM. Furthermore, our observation of *BCL2* promoter hypermethylation with mRNA downregulation indicates an additional epigenetic mechanism may confer resistance to venetoclax in *MYD88*^{WT} WM, which has been predominantly evaluated in patients with *MYD88*^{MUT} disease (9).

Overall, the results of this study offer novel insights into the biology of *MYD88*^{WT} WM, suggest its epigenetic distinction from *MYD88*^{MUT} WM, and propose how DNA methylation and non-coding RNAs may contribute to the unique clinical phenotype of patients with this disease. Some of the key epigenetic findings identified, such as the non-coding downregulation of cytokine and inflammatory signaling pathways, may play a role in the inferior outcomes and reduced response to conventional WM-directed therapies in patients with *MYD88*^{WT} WM. Larger studies are needed to investigate the epigenetic similarities between *MYD88*^{WT} WM and other B-cell lymphomas, including marginal zone lymphoma, which may help to improve biological subclassification. Furthermore, functional studies are needed to validate these findings at the proteomic level and explore the potential utility of epigenetic therapies for the treatment of *MYD88*^{WT} WM.

References

1. Treon SP, Xu L, Yang G, et al. MYD88 L265P somatic mutation in Waldenstrom's macroglobulinemia. N Engl J Med. 2012;367(9):826-833.

2. Varettoni M, Arcaini L, Zibellini S, et al. Prevalence and clinical significance of the MYD88 (L265P) somatic mutation in Waldenstrom's macroglobulinemia and related lymphoid neoplasms. Blood. 2013;121(13):2522-2528.

3. Zanwar S, Abeykoon JP, Durot E, et al. Impact of MYD88(L265P) mutation status on histological transformation of Waldenstrom Macroglobulinemia. Am J Hematol. 2020;95(3):274-281.

4. Yang H, Green MR. Harnessing lymphoma epigenetics to improve therapies. Blood. 2020;136(21):2386-2391.

5. Chohan K, Paludo J, Dasari S, et al. MicroRNA and long non-coding RNA analysis in IgM-monoclonal gammopathies reveals epigenetic influence on cellular functions and oncogenesis. Haematologica. 2024;109(5):1570-1575.

6. Chohan K, Paludo J, Dasari S, et al. Multiomics analysis of IgM monoclonal gammopathies reveals epigenetic influence on oncogenesis via DNA methylation. Blood. 2024;144(12):1284-1289.

7. Mondello P, Paludo J, Novak JP, et al. Molecular Clusters and Tumor-Immune Drivers of IgM Monoclonal Gammopathies. Clin Cancer Res. 2023;29(5):957-970.

8. Elsawa SF, Novak AJ, Ziesmer SC, et al. Comprehensive analysis of tumor microenvironment cytokines in Waldenstrom macroglobulinemia identifies CCL5 as a novel modulator of IL-6 activity. Blood. 2011;118(20):5540-5549.

9. Castillo JJ, Allan JN, Siddiqi T, et al. Venetoclax in Previously Treated Waldenstrom Macroglobulinemia. J Clin Oncol. 2022;40(1):63-71.

10. Lawson CD, Burridge K. The on-off relationship of Rho and Rac during integrin-mediated adhesion and cell migration. Small GTPases. 2014;5:e27958.

11. Akhlaghipour I, Moghbeli M. MicroRNA-98 as a novel diagnostic marker and therapeutic target in cancer patients. Discov Oncol. 2024;15(1):385.

12. Yeh M, Wang Y-Y, Yoo JY, et al. MicroRNA-138 suppresses glioblastoma proliferation through downregulation of CD44. Sci Rep. 2021;11(1):9219.

13. Wong M, Polly P, Liu T. The histone methyltransferase DOT1L: regulatory functions and a cancer therapy target. Am J Cancer Res. 2015;5(9):2823-2837.

14. Yang L, Rau R, Goodell MA. DNMT3A in haematological malignancies. Nat Rev Cancer. 2015;15(3):152-165.

15. Hunter ZR, Xu L, Tsakmaklis N, et al. Insights into the genomic landscape of MYD88 wild-type Waldenstrom macroglobulinemia. Blood Adv. 2018;2(21):2937-2946.

Table I. Patient characteristics of WM samples

Parameter	All Patients (n=15)	*MYD88*^{MUT} WM (n=12)	*MYD88*^{WT} WM (n=3)	p
Age at diagnosis, years	60 (46-76)	61 (49-76)	48 (46-60)	0.07
Male sex, n (%)	9 (60)	7 (58)	2 (67)	0.79
Hemoglobin, g/dL	12.2 (9.5-15.8)	12.0 (9.5-15.8)	12.7 (11.1-13.4)	0.72
Platelets, x10^9/L	213 (96-512)	193 (96-512)	242 (213-348)	0.68
B2 microglobulin, mcg/mL	3.01 (1.64-5.91)	3.07 (1.64-5.91)	3.04 (1.75-3.07)	0.35
IgM, mg/dL	2240 (173-10000)	2790 (173-10000)	1400 (604-3400)	0.43
BM involvement, %	50 (10-90)	50 (10-90)	20 (20-40)	0.15
Abnormal FLC ratio, n (%)	3 (23)	3 (30%)	0	0.28
CXCR4 Mutated n (%)	3 (20)	3 (25%)	0	0.33
Dx to LFU, mos (range)	87.4 (29.4-142.3)	91.0 (29.4-142.3)	80.0 (47.6-92.2)	0.63

All characteristics at the time of sample collection. B2, beta-2; BM, bone marrow; Dx, diagnosis; IgM, immunoglobulin M; LFU, last follow-up; mos, months; n, number. FLC data was available in 13 patients (WT: 3; MUT: 10). Unless specified, values represent medians (range).

Figure Legends:

Figure 1. Genome-wide methylation analyses with promoter-methylation-based pathway integration. Analysis evaluating differentially methylated regions (DMRs) comparing *MYD88*^{WT} WM to controls (A) and methylation-based pathway analysis evaluating promoter methylation and mRNA expression (B). DMR analysis comparing *MYD88*^{WT} to *MYD88*^{MUT} WM (C) with corresponding pathway analysis (D). IL-8 pathway analysis demonstrating downstream involvement of RHOC and RRAS2 (E).

Figure 2. MicroRNA (miRNA) differential expression with miRNA-based pathway analysis. Volcano-plot demonstrating miRNA differential expression in *MYD88*^{WT} WM to controls (A) and miRNA-based pathway analysis integrating mRNA differential expression (B). miRNA differential expression comparing *MYD88*^{WT} to *MYD88*^{MUT} WM (C) with miRNA-based pathway analysis (D). Postulated mechanism whereby downregulation of miR-138-5p permits increased DNMT3A expression and consequent CpG hypermethylation (E).

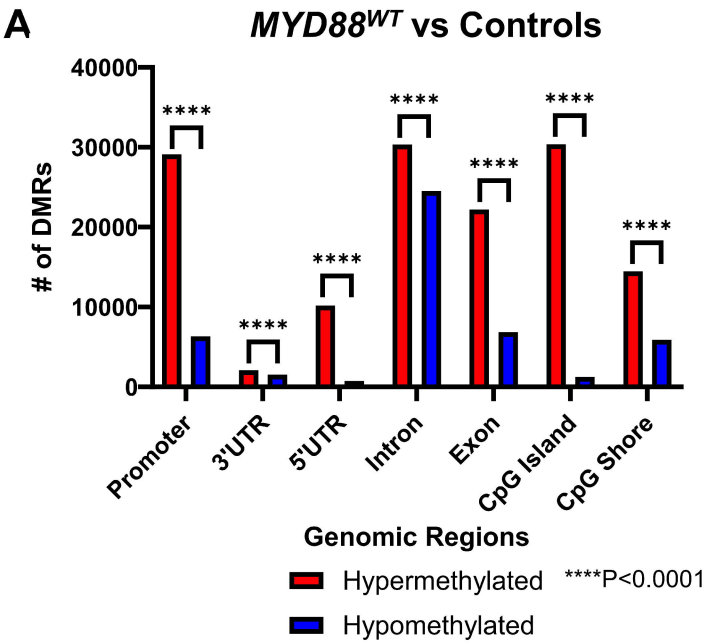
A
MYD88WT vs Controls
# of DMRs
40000
30000
20000
10000
0
****
Promoter
3'UTR
5'UTR
Intron
Exon
CpG Island
CpG Shore
Genomic Regions
Hypermethylated
Hypomethylated
****P<0.0001

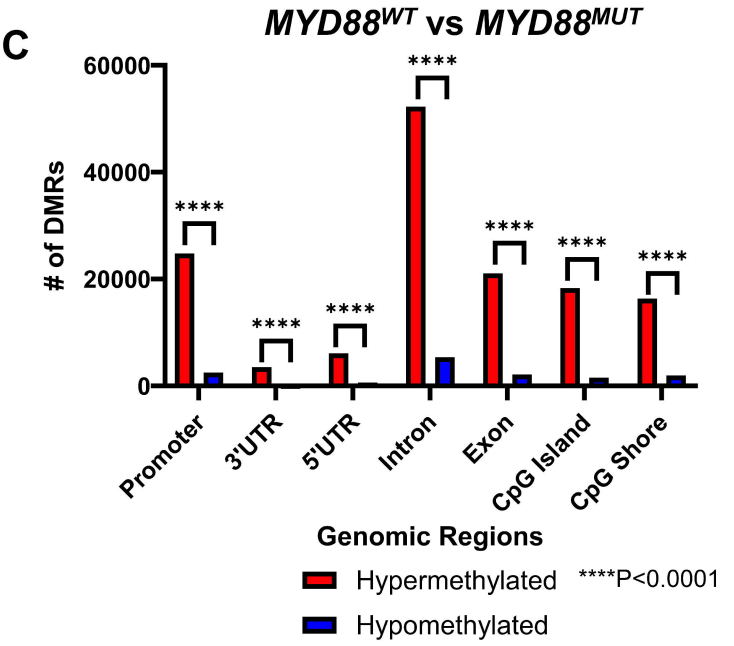
C
MYD88WT vs MYD88MUT
# of DMRs
60000
40000
20000
0
****
Promoter
3'UTR
5'UTR
Intron
Exon
CpG Island
CpG Shore
Genomic Regions
Hypermethylated
Hypomethylated
****P<0.0001

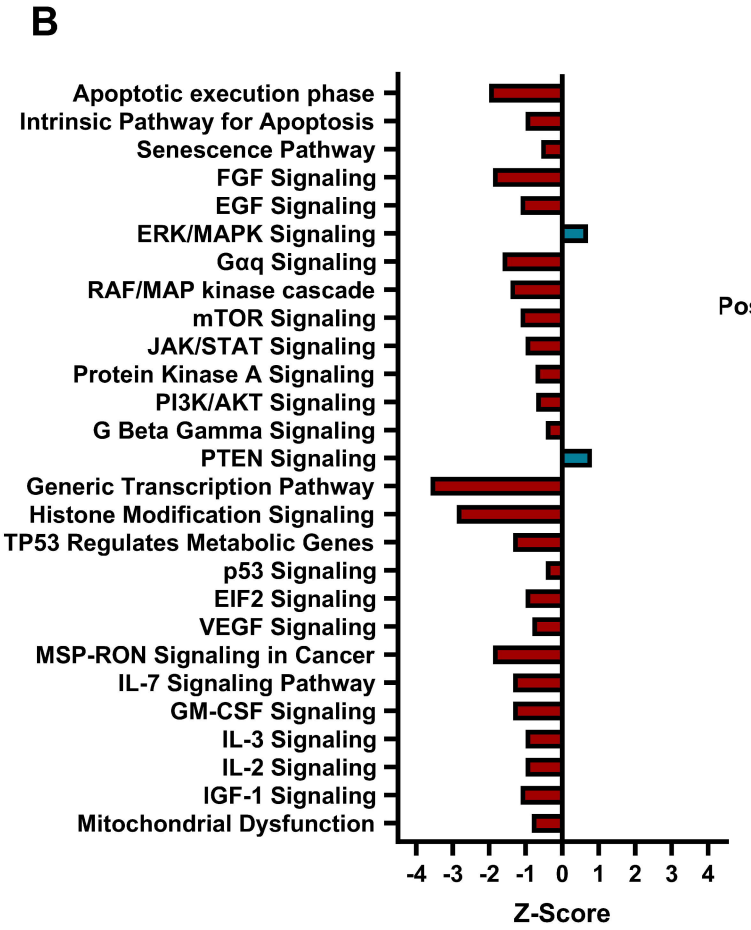
B
Apoptotic execution phase
Intrinsic Pathway for Apoptosis
Senescence Pathway
FGF Signaling
EGF Signaling
ERK/MAPK Signaling
Gαq Signaling
RAF/MAP kinase cascade
mTOR Signaling
JAK/STAT Signaling
Protein Kinase A Signaling
PI3K/AKT Signaling
G Beta Gamma Signaling
PTEN Signaling
Generic Transcription Pathway
Histone Modification Signaling
TP53 Regulates Metabolic Genes
p53 Signaling
EIF2 Signaling
VEGF Signaling
MSP-RON Signaling in Cancer
IL-7 Signaling Pathway
GM-CSF Signaling
IL-3 Signaling
IL-2 Signaling
IGF-1 Signaling
Mitochondrial Dysfunction
-4 -3 -2 -1 0 1 2 3 4
Z-Score

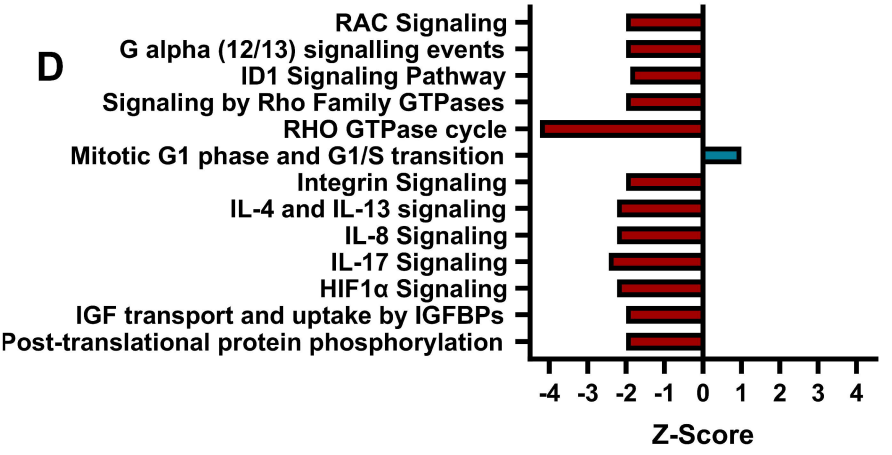
D
RAC Signaling
G alpha (12/13) signalling events
ID1 Signaling Pathway
Signaling by Rho Family GTPases
RHO GTPase cycle
Mitotic G1 phase and G1/S transition
Integrin Signaling
IL-4 and IL-13 signaling
IL-8 Signaling
IL-17 Signaling
HIF1α Signaling
IGF transport and uptake by IGFBPs
Post-translational protein phosphorylation
-4 -3 -2 -1 0 1 2 3 4
Z-Score

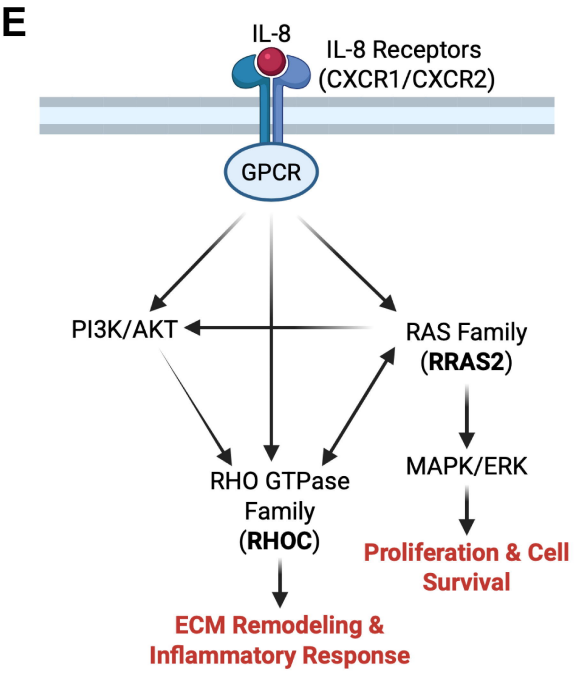
E
IL-8
IL-8 Receptors
(CXCR1/CXCR2)
GPCR
PI3K/AKT
RAS Family
(RRAS2)
RHO GTPase
Family
(RHOC)
MAPK/ERK
Proliferation & Cell
Survival
ECM Remodeling &
Inflammatory Response

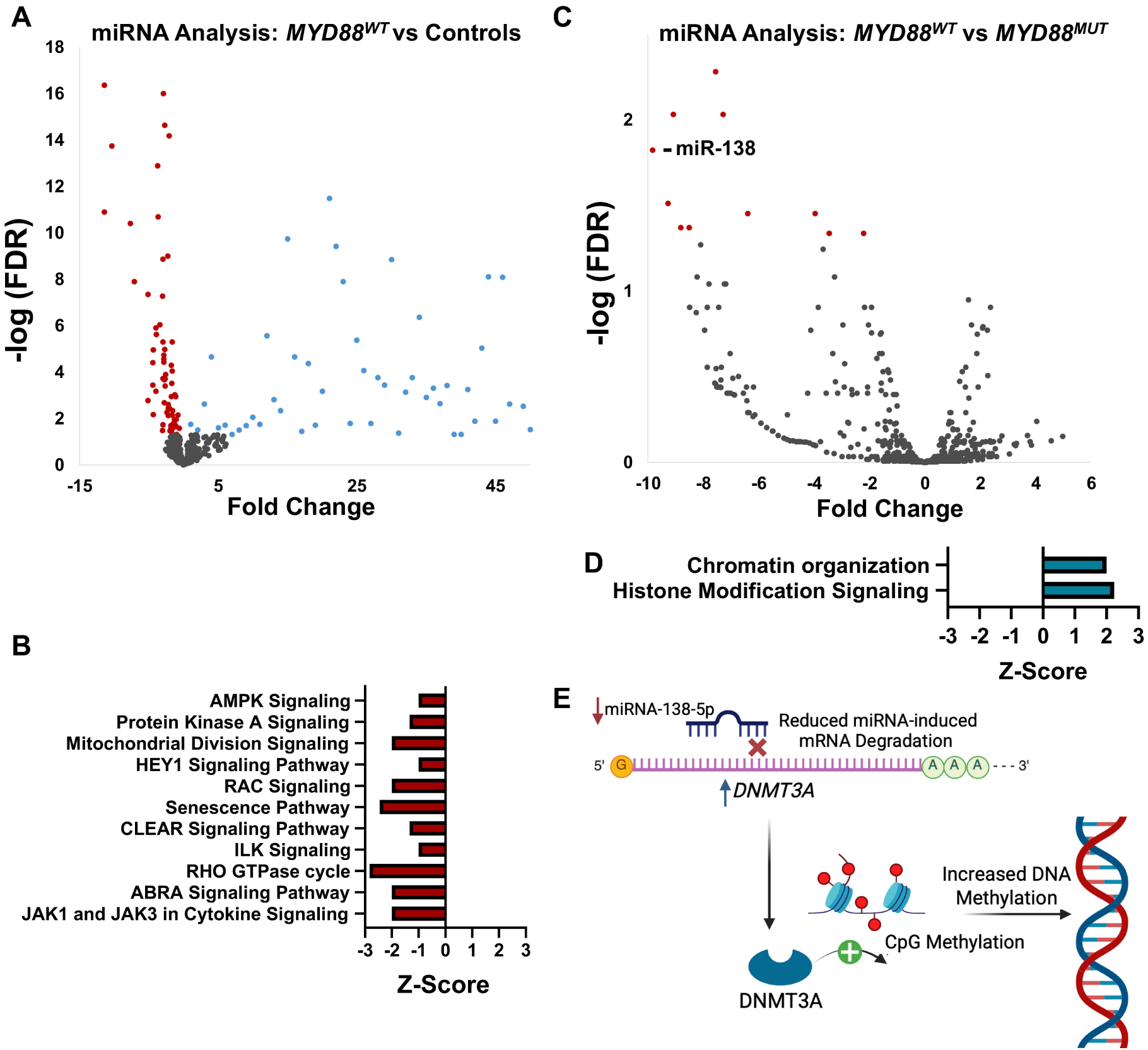
A
miRNA Analysis: MYD88WT vs Controls
-log (FDR)
Fold Change
C
miRNA Analysis: MYD88WT vs MYD88MUT
miR-138
-log (FDR)
Fold Change
D
Chromatin organization
Histone Modification Signaling
Z-Score
B
AMPK Signaling
Protein Kinase A Signaling
Mitochondrial Division Signaling
HEY1 Signaling Pathway
RAC Signaling
Senescence Pathway
CLEAR Signaling Pathway
ILK Signaling
RHO GTPase cycle
ABRA Signaling Pathway
JAK1 and JAK3 in Cytokine Signaling
Z-Score
E
miRNA-138-5p
Reduced miRNA-induced mRNA Degradation
5'
G
A A A
3'
DNMT3A
Increased DNA Methylation
CpG Methylation
DNMT3A

Supplemental Material

Article Title: Multi-omics analysis reveals a unique epigenetic signature in *MYD88* wild-type Waldenstrom macroglobulinemia

Running Header: DNA methylation in *MYD88*-WT WM

Authors: Karan Chohan[1#], Jonas Paludo[1#], Surendra Dasari[2], Joseph P Novak[1], Jithma P. Abeykoon[1], Saurabh Zanwar[1], Zhi-Zhang Yang[1], Shahrzad Jalali[1], Vaishali Bhardwaj[1], Jordan E Krull[1], Esteban Braggio[3], Michelle K. Manske[1], Craig B. Reeder[4], Sikander Ailawadhi[4], Asher Chanan-Khan[4], Prashant Kapoor[1], Robert A. Kyle[1], Morie A Gertz[1], Anne J. Novak[1], Patrizia Mondello[1] and Stephen M. Ansell[1*]

[1]Division of Hematology, Mayo Clinic, Rochester, MN

[2]Department of Health Sciences Research, Mayo Clinic, Rochester, MN

[3]Division of Hematology and Medical Oncology, Mayo Clinic, Scottsdale, AZ

[4]Division of Hematology and Oncology, Mayo Clinic, Jacksonville, FL

#Authors contributed equally

***Corresponding Author:**

Stephen M. Ansell, M.D., Ph.D.

200 1st ST SW, Rochester, MN, USA, 55902

Email: ansell.stephen@mayo.edu; Phone: (507)-284-2511

Supplemental Table 1: Gene set enrichment analysis evaluating RNA expression comparing patients with *MYD88*^{WT} to *MYD88*^{MUT} WM. Only top 20 positively and negatively enriched pathways are displayed. Normalized enrichment score (NES) and false discovery rate (FDR) indicated per pathway. FDR<0.001 indicated as 0.

NAME	NES	FDR
HALLMARK_E2F_TARGETS	2.86	0
HALLMARK_MYC_TARGETS_V1	2.65	0
REACTOME_SYNTHESIS_OF_DNA	2.47	0
REACTOME_G2_M_CHECKPOINTS	2.46	0
REACTOME_CELL_CYCLE_MITOTIC	2.41	0
HALLMARK_G2M_CHECKPOINT	2.40	0
REACTOME_THE_ROLE_OF_GTSE1_IN_G2_M_PROGRESSION_AFTER_G2_CHECKPOINT	2.40	0
REACTOME_DNA_REPLICATION	2.40	0
REACTOME_CELL_CYCLE_CHECKPOINTS	2.39	0
REACTOME_ABC_TRANSPORTER_DISORDERS	2.38	0
REACTOME_S_PHASE	2.38	0
REACTOME_SCF_SKP2_MEDIATED_DEGRADATION_OF_P27_P21	2.38	0
REACTOME_MITOTIC_G2_G2_M_PHASES	2.38	0
REACTOME_DEFECTIVE_CFTR_CAUSES_CYSTIC_FIBROSIS	2.36	0
REACTOME_SCF_BETA_TRCP_MEDIATED_DEGRADATION_OF_EMI1	2.36	0
REACTOME_APC_C_MEDIATED_DEGRADATION_OF_CELL_CYCLE_PROTEINS	2.33	0
REACTOME_NEGATIVE_REGULATION_OF_NOTCH4_SIGNALING	2.31	0
REACTOME_TRANSCRIPTIONAL_REGULATION_BY_RUNX2	2.31	0
REACTOME_AUF1_HNRNP_D0_BINDS_AND_DESTABILIZES_MRNA	2.31	0
REACTOME_CHROMOSOME_MAINTENANCE	2.30	0
HALLMARK_TNFA_SIGNALING_VIA_NFKB	-2.31	0
KEGG_CYTOKINE_CYTOKINE_RECEPTOR_INTERACTION	-2.30	0
KEGG_HEMATOPOIETIC_CELL_LINEAGE	-2.04	0.001
BIOCARTA_TOB1_PATHWAY	-2.04	0.001
HALLMARK_COMPLEMENT	-2.03	0.002
KEGG_GRAFT_VERSUS_HOST_DISEASE	-2.02	0.002
HALLMARK_ALLOGRAFT_REJECTION	-1.96	0.007
KEGG_INTESTINAL_IMMUNE_NETWORK_FOR_IGA_PRODUCTION	-1.94	0.008
BIOCARTA_INFLAM_PATHWAY	-1.92	0.011
HALLMARK_INFLAMMATORY_RESPONSE	-1.92	0.010
KEGG_ALLOGRAFT_REJECTION	-1.92	0.010
KEGG_TYPE_I_DIABETES_MELLITUS	-1.88	0.017
BIOCARTA_CTLA4_PATHWAY	-1.88	0.016
REACTOME_KIDNEY_DEVELOPMENT	-1.86	0.021
REACTOME_COSTIMULATION_BY_THE_CD28_FAMILY	-1.85	0.024
REACTOME_CHEMOKINE_RECEPTORS_BIND_CHEMOKINES	-1.84	0.023
HALLMARK_IL6_JAK_STAT3_SIGNALING	-1.84	0.023
KEGG_AUTOIMMUNE_THYROID_DISEASE	-1.83	0.026
REACTOME_RAC1_GTPASE_CYCLE	-1.82	0.029
BIOCARTA_ALK_PATHWAY	-1.82	0.028